

Non-equilibrium transitions in fully frustrated Josephson junction arrays

Verónica I. Marconi and Daniel Domínguez

Centro Atómico Bariloche, 8400 S. C. de Bariloche, Río Negro, Argentina

We study the effect of thermal fluctuations in a fully frustrated Josephson junction array driven by a current I larger than the apparent critical current $I_c(T)$. We calculate numerically the behavior of the chiral order parameter of Z_2 symmetry and the transverse helicity modulus (related to the $U(1)$ symmetry) as a function of temperature. We find that the Z_2 transition occurs at a temperature $T_{Z_2}(I)$ which is lower than the temperature $T_{U(1)}(I)$ for the $U(1)$ transition. Both transitions could be observed experimentally from measurements of the longitudinal and transverse voltages.

PACS numbers: 74.50+r, 74.60.Ge, 74.60.Ec

The study of non-equilibrium steady states of driven many-degrees-of-freedom systems are of importance in condensed matter physics [1–4]. Examples of this problem are the dynamics of vortices in type II superconductors [1–3] and charge density waves [4]. In two dimensions, Josephson junction arrays (JJA) are a well controlled system [5] where this issue can be investigated [6,7]. In the presence of a magnetic field such that there is a half flux quantum per plaquette, $f = Ha^2/\Phi_0 = 1/2$, the JJA corresponds to the fully frustrated XY (FFXY) model [8–11]. The ground state is a “checkerboard” vortex lattice, in which a vortex sits in every other site of an square grid [8]. There are two types of competing order and broken symmetries: the discrete Z_2 symmetry of the ground state of the vortex lattice, with an associated chiral (Ising-like) order parameter, and the continuous $U(1)$ symmetry associated with superconducting phase coherence. The critical behavior of this system has been the subject of several experimental [10] and theoretical [8,9,11–16] studies. There are a Z_2 transition (Ising-like) and a $U(1)$ transition (Kosterlitz-Thouless-like) with critical temperatures $T_{Z_2} \geq T_{U(1)}$. There is a controversy about these temperatures being extremely close [14] or equal [13,15,16]. In the light of this, it is worth studying the possibility of non-equilibrium Z_2 and $U(1)$ transitions at large driving currents. Also, the dynamical transitions in driven systems studied up to now [1–4,6,7] involve continuous (translational or gauge) symmetries, and therefore it is interesting to study a system with a discrete symmetry. Previously, we have found dynamical transitions of the vortex lattice in a JJA with a field density of $f = 1/25$ [7]: for large currents I there is a melting transition of the moving vortex lattice at a temperature higher than the transverse superconducting transition: $T_M(I) > T_{U(1)}(I)$. Interestingly, here we find that the opposite case occurs in the driven FFXXY: the order of the “checkerboard” vortex lattice is destroyed at a much lower temperature than the transverse superconducting coherence, $T_{Z_2}(I) < T_{U(1)}(I)$.

The hamiltonian of the frustrated XY model is:

$$\mathcal{H} = - \sum_{\mu, \mathbf{n}} \frac{\Phi_0 I_0}{2\pi} \cos[\theta(\mathbf{n} + \mu) - \theta(\mathbf{n}) - A_\mu(\mathbf{n})], \quad (1)$$

where I_0 is the critical current of the junction between the sites \mathbf{n} and $\mathbf{n} + \mu$ in a square lattice [$\mathbf{n} = (n_x, n_y)$, $\mu = \hat{\mathbf{x}}, \hat{\mathbf{y}}$], R_N is the normal state resistance and $\theta_\mu(\mathbf{n}) = \theta(\mathbf{n} + \mu) - \theta(\mathbf{n}) - A_\mu(\mathbf{n}) = \Delta_\mu \theta(\mathbf{n}) - A_\mu(\mathbf{n})$ is the gauge invariant phase difference with $A_\mu(\mathbf{n}) = \frac{2\pi}{\Phi_0} \int_{\mathbf{n}a}^{(\mathbf{n}+\mu)a} \mathbf{A} \cdot d\mathbf{l}$. In the presence of an external magnetic field H we have $\Delta_\mu \times A_\mu(\mathbf{n}) = A_x(\mathbf{n}) - A_x(\mathbf{n} + \mathbf{y}) + A_y(\mathbf{n} + \mathbf{x}) - A_y(\mathbf{n}) = 2\pi f$, $f = Ha^2/\Phi_0$ and a is the array lattice spacing. For a fully frustrated JJA we have $f = 1/2$. Here, we will take periodic boundary conditions (p.b.c) in both directions in the presence of an external current I_{ext} in arrays with $L \times L$ junctions [6]. The vector potential is taken as $A_\mu(\mathbf{n}, t) = A_\mu^0(\mathbf{n}) - \alpha_\mu(t)$ where in the Landau gauge $A_x^0(\mathbf{n}) = -2\pi f n_y$, $A_y^0(\mathbf{n}) = 0$ and $\alpha_\mu(t)$ will allow for total voltage fluctuations. With this gauge the p.b.c. for the phases are: $\theta(n_x + L, n_y) = \theta(n_x, n_y)$ and $\theta(n_x, n_y + L) = \theta(n_x, n_y) - 2\pi f L n_x$. The current flowing in the junction between two superconducting islands in a JJA is modeled as the sum of the Josephson and the normal currents [6,7,11,17]:

$$I_\mu(\mathbf{n}) = I_0 \sin \theta_\mu(\mathbf{n}) + \frac{\Phi_0}{2\pi c R_N} \frac{\partial \theta_\mu(\mathbf{n})}{\partial t} + \eta_\mu(\mathbf{n}, t) \quad (2)$$

where the thermal noise fluctuations η_μ have correlations $\langle \eta_\mu(\mathbf{n}, t) \eta_{\mu'}(\mathbf{n}', t') \rangle = \frac{2kT}{R_N} \delta_{\mu, \mu'} \delta_{\mathbf{n}, \mathbf{n}'} \delta(t - t')$. The condition of a current flowing in the y -direction: $\sum_{\mathbf{n}} I_\mu(\mathbf{n}) = I_{ext} L^2 \delta_{\mu, y}$ determines the dynamics of $\alpha_\mu(t)$ [6,7]. After considering local conservation of current, $\Delta_\mu \cdot I_\mu(\mathbf{n}) = \sum_{\mu} I_\mu(\mathbf{n}) - I_\mu(\mathbf{n} - \mu) = 0$, we obtain the full RSJ-Langevin dynamical equations of the driven XY model as in [6,7]. We normalize currents by I_0 , time by $\tau_J = 2\pi c R_N I_0 / \Phi_0$ and temperature by $I_0 \Phi_0 / 2\pi k_B$. We solve the dynamical equations with time step $\Delta t = 0.001 - 0.1 \tau_J$ and integration times $10000 \tau_J$ after a transient of $5000 \tau_J$.

We study the fully frustrated JJA for system sizes of $L \times L$ junctions, with $L = 8, 16, 24, 32, 48, 64, 128$. In the absence of external currents, we find an equilibrium phase transition at $T_c = 0.45$ which, within a resolution of $\Delta T = 0.005$, corresponds to a simultaneous (or very close) breaking of the $U(1)$ and the Z_2 symmetries. Here we will analyze the possible occurrence of these transitions as a function of temperature when the JJA is driven

by currents well above the zero temperature critical current $I > I_{c0} = (\sqrt{2} - 1)I_0 \approx 0.414I_0$.

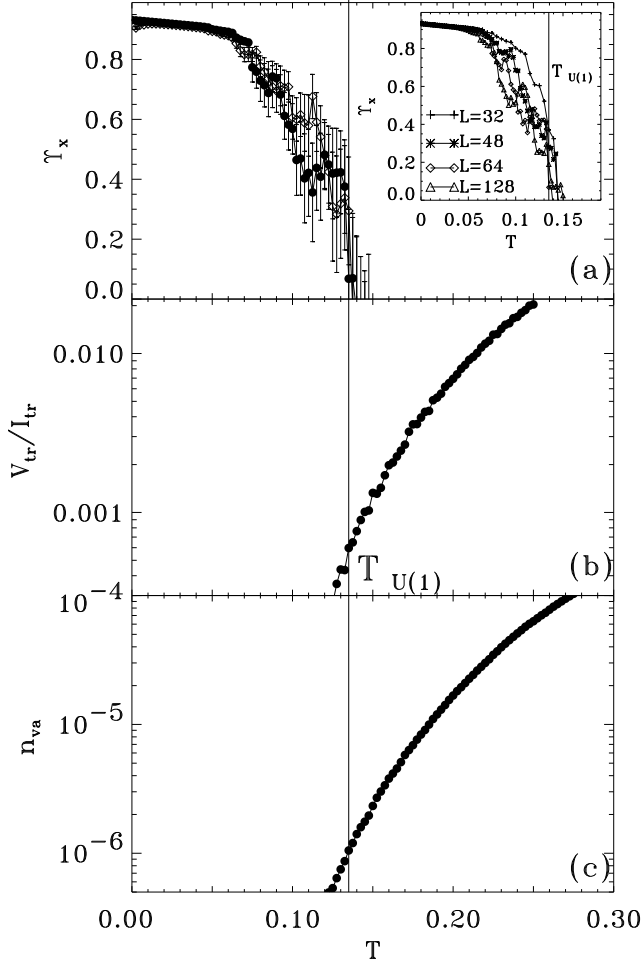


FIG. 1. Breaking of the $U(1)$ symmetry for a large current: $I = 0.9$, $I > I_c(0)$, system size 64×64 . a) Helicity Modulus Υ_x vs temperature T (\bullet increasing T , \diamond decreasing T). Inset: size effect for $L = 32, 48, 64, 128$. b) Transverse voltage for a small transverse current, $I_{tr} = 0.1$, vs T . c) Vortex-antivortex pairs density, n_{va} vs. T .

$U(1)$ symmetry and transverse superconductivity. In the driven JJA superconducting coherence can only be defined in the direction transverse to the bias current [7,18]. We calculate the transverse helicity modulus $\Upsilon_x = \frac{1}{L^2} \langle \sum_{\mathbf{n}} \cos \theta_x(\mathbf{n}) \rangle - \frac{1}{T} \frac{1}{L^4} \{ \langle [\sum_{\mathbf{n}} \sin \theta_x(\mathbf{n})]^2 \rangle - \langle [\sum_{\mathbf{n}} \sin \theta_x(\mathbf{n})] \rangle^2 \}$. [In order to calculate the helicity modulus along x , we enforce strict periodicity in θ by fixing $\alpha_x(t) = 0$]. We find that Υ_x is finite at low T and vanishes at a temperature $T_{U(1)}(I)$. In Fig.1a we show the behavior of $\Upsilon_x(T)$ for a current $I = 0.9$ in a 64×64 JJA. The inset of Fig.1a shows Υ_x for sizes $L = 32, 48, 64, 128$, we see that a transition temperature can be defined independently of lattice size. This transition is reversible: we obtain the same behavior when decreasing T from a random configuration at $T = 1$ and when increasing T

from an ordered state at $T = 0$, see Fig.1a.

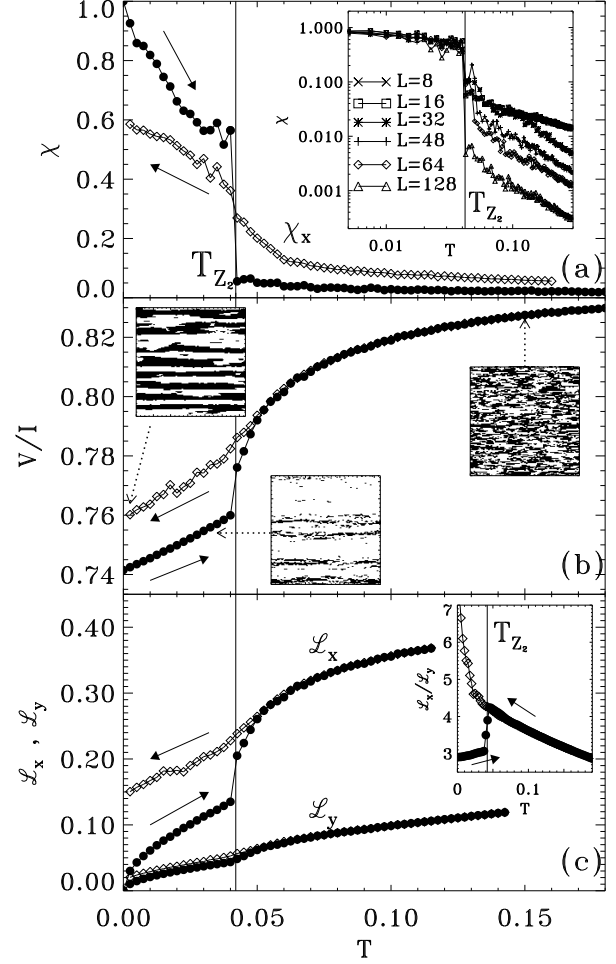


FIG. 2. Breaking of the Z_2 symmetry for a large current: $I = 0.9$, $I > I_c(0)$, system size 128×128 , results for increasing T (\bullet) and decreasing T (\diamond). a) Chiral order parameter χ vs T and one-dimensional order parameter χ_x vs. T . Inset: size effect for χ for $L = 8, 16, 32, 48, 64, 128$. b) Longitudinal voltage V vs. T . Insets: snapshots of the staggered magnetization $m_s(\mathbf{n}, t)$: ordered state for $T = 0.035$ (warming up), high temperature disordered state, $T = 0.15$, and low temperature state with \mathcal{L}_x -domain walls, $T = 0.0025$ (cooling down). c) Domain wall lengths \mathcal{L}_x and \mathcal{L}_y vs. T . Inset: domain anisotropy $\mathcal{L}_x/\mathcal{L}_y$ vs. T .

Transverse superconductivity can be measured when a small current I_{tr} is applied perpendicular to the driving current: we find a vanishingly small transverse voltage V_{tr} below $T_{U(1)}(I)$, as we found before in [7] for $f = 1/25$. We obtain the voltage in the μ -direction as the time average $V_\mu = \langle d\alpha_\mu(t)/dt \rangle$ (normalized by $R_N I_0$); longitudinal voltage is $V = V_y$ and transverse voltage is $V_{tr} = V_x$. In Fig.1b we see that the transverse resistance V_{tr}/I_{tr} is negligibly small for $T < T_{U(1)}$ and starts to rise near the transition. The equilibrium $U(1)$ transition (at $f = 0$, $I = 0$, Kosterlitz-Thouless) is characterized by the un-

binding of vortex-antivortex pairs above T_c . We calculate the density n_{va} of vortex-antivortex excitations above checkerboard vortex configuration as $2n_{va} = \langle |b(\tilde{\mathbf{n}})| \rangle - f$, where the vorticity at the plaquette $\tilde{\mathbf{n}}$ (associated to the site \mathbf{n}) is $b(\tilde{\mathbf{n}}) = -\Delta_\mu \times \text{nint}[\theta_\mu(\mathbf{n})/2\pi]$. We see in Fig.1c that n_{va} rises near $T_{U(1)}$. Moreover, the transverse resistivity above $T_{U(1)}$ is $V_{tr}/I_{tr} \propto n_{va}$.

Z_2 symmetry. Since the ground state is a checkerboard pattern of vortices, we define the “staggered magnetization” as $m_s(\tilde{\mathbf{n}}, t) = (-1)^{n_x+n_y}[2b(n_x, n_y, t) - 1]$ and $m_s(t) = (1/L^2) \sum_{\tilde{\mathbf{n}}} m_s(\tilde{\mathbf{n}}, t)$. At $T = 0$, $I = 0$ there are two degenerate configurations with $m_s = \pm 1$. Above the $T = 0$ critical current I_{c0} the checkerboard state moves as a rigid structure and $m_s(t)$ changes sign periodically with time. Therefore we define the chiral order parameter as $\chi = \langle m_s^2(t) \rangle$. We start the simulation at $T = 0$ with an ordered checkerboard state driven by a current $I > I_{c0}$ and then we increase slowly the temperature. We obtain that the chirality parameter vanishes at a temperature T_{Z_2} , which is smaller than $T_{U(1)}$, as can be seen in Fig.2a for $I = 0.9$. This transition is confirmed by the size analysis shown in the inset of Fig.2a: for $T < T_{Z_2}$ the chirality χ is independent of size, while for $T > T_{Z_2}$ we see that $\chi \sim 1/L^2$. As it is shown in Fig.2b, the longitudinal voltage V has a sharp increase at T_{Z_2} , which could be easily detected experimentally. The excitations that characterize the Z_2 transition are domain walls that separate domains with different signs of m_s . The length of domain walls in the direction μ is given by $\mathcal{L}_\mu = (2/L^2) \sum_{\tilde{\mathbf{n}}} \langle b(\tilde{\mathbf{n}})b(\tilde{\mathbf{n}} + \nu) \rangle$, with $\nu \perp \mu$. We find that for $I > 0$ and $T > 0$ the domains are anisotropic, with the domain walls being longer in the direction perpendicular to the current ($\mathcal{L}_x > \mathcal{L}_y$) and the domain anisotropy $\mathcal{L}_x/\mathcal{L}_y$ increasing with I . In Fig.2c we show the dependence of \mathcal{L}_μ with temperature for $I = 0.9$. At $T = 0$ there are no domain walls, since the initial condition is the checkerboard state, and the domain wall length grows with T , showing a sharp increase at T_{Z_2} . The domain anisotropy $\mathcal{L}_x/\mathcal{L}_y$ is shown in the inset of Fig.2c: it has a clear jump at the transition in T_{Z_2} while for $T \gg T_{Z_2}$ the domains tend to be less anisotropic. When decreasing temperature from a random configuration at $T = 1$, an important number of domain walls along the x direction remain frozen below T_{Z_2} : \mathcal{L}_x tends to a finite value when $T \rightarrow 0$ and the domain anisotropy tends to diverge when cooling down. This leads to a strong hysteresis in the voltage V at T_{Z_2} (see Fig.2b) since the extra domain walls increase dissipation [11,19]. This low T state with frozen-in domain walls is ordered along the x -direction (i.e. perpendicular to I) but is disordered along the y direction which gives $\chi \approx 0$. We define the Z_2 order parameter in the x direction as $\chi_x = \langle (1/L) \sum_{n_y} [(1/L) \sum_{n_x} m_s(n_x, n_y, t)]^2 \rangle$ and χ_y is defined analogously. We see in Fig.2a that, when cooling down from high T , χ_x vanishes as $\chi_x \sim 1/L$ for $T > T_{Z_2}$ (it has stronger size effects than χ) and becomes

finite for $T < T_{Z_2}$, while $\chi_y \approx 0$ for any T . Therefore, depending on the history, there are two kinds of high current steady states with broken Z_2 symmetry at low T , examples of which are shown in the inset of Fig.2b. One state has mostly the checkerboard structure ($\chi \neq 0$) with few very anisotropic domains. It can be obtained experimentally by cooling down at zero drive and then increasing I . The other steady state is ordered in the direction perpendicular to I ($\chi_x \neq 0$, $\chi_y = 0$) with several domain walls along the x direction. These domain walls move in the direction parallel to I (via the motion of vortices perpendicular to I) giving an additional dissipation. This state can be obtained experimentally by cooling down with a fixed I .

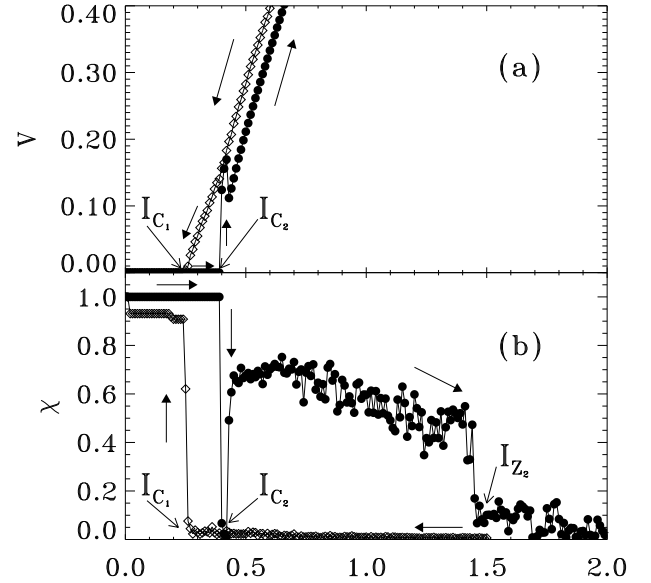


FIG. 3. Current-voltage hysteresis for $T = 0.02$ shown for (a) voltage vs. I and (b) chiral order parameter vs. I . Increasing current from the checkerboard state (\bullet) and decreasing current from a random state at large $I > I_{Z_2}$ (\diamond).

The two steady states have also different critical currents as can be observed in the low T current-voltage (IV) characteristics. In Fig.3a we show the IV curve for $T = 0.02$ and in Fig.3b the corresponding χ vs. I curve. When increasing I from the $I = 0$ equilibrium state, we find a critical current $I_{c2}(T)$, which in the limit of $T = 0$ tends to $I_{c0} = \sqrt{2} - 1$ as found analytically and in simulations with p.b.c [8,20,21]. Near I_{c2} the order parameter χ has a minimum and rapidly increases with I . The driven state is an ordered state similar to the one shown in Fig.2b. At a higher current I_{Z_2} there is a sharp drop of χ which corresponds to the crossing of the $T_{Z_2}(I)$ line (see Fig.4) and the Z_2 order is lost. If we now decrease the current either from the disordered state at $I > I_{Z_2}$ or from a random initial configuration or from a configuration cooled down at a fixed $I > I_{c2}$, we obtain the steady state with domain walls along the x direction and

$\chi \approx 0, \chi_x \neq 0$. This state has a higher voltage and pins at a lower critical current $I_{c1}(T)$, which has the $T = 0$ limit $I_{c1}(T \rightarrow 0) = 0.35$. It has been shown recently [21] that open boundary conditions can nucleate domain walls leading to the critical current $I_{c1}(0) = 0.35$ usually found in open boundary $T = 0$ simulations [11,17,19]. Also a moving state with parallel domain walls (as in the inset of Fig.3b) has been found by Grønbech-Jensen *et al.* [22] in $f = 1/2$ JJA with open boundaries and Marino and Halsey [23] have shown that the high current states of frustrated JJA can have moving domain walls. We have studied the effect of open boundaries in the direction of I , in the direction perpendicular to I and in both directions. They differ mainly in the $T = 0$ critical current and IV curve, for finite T there are small differences in the detailed shape of the hysteresis in critical current. In all the cases the two high current steady states are observed at finite T with the same history dependence. Also, we find that the density of frozen \mathcal{L}_x domain walls depends on cooling rate and decreases with system size.

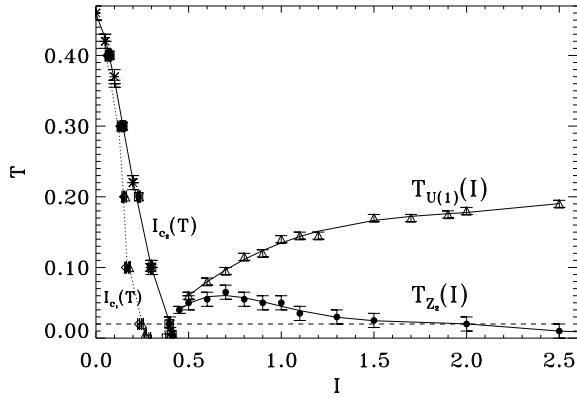


FIG. 4. Current-temperature phase diagram. $T_{U(1)}(I)$ line obtained from $\Upsilon_x(T)$ and $V_{tr}(T)$ (Δ). $T_{Z_2}(I)$ line obtained from $\chi(T)$, $V(T)$ and $\mathcal{L}_x/\mathcal{L}_y(T)$ (\bullet). $I_{c1}(T)$ (\diamond) and $I_{c2}(T)$ (\bullet) are obtained from hysteresis in IV curves as well as from hysteresis in $\Upsilon_x(T)$ and $\chi(T)$ curves. The dashed line corresponds to the IV curve of Fig.3 ($T = 0.02$).

In summary, we have obtained the current-temperature phase diagram of the driven fully frustrated XY model, which is shown in Fig.4. At high currents the breaking of the $U(1)$ and the Z_2 symmetries occurs at well separated temperatures, with $T_{Z_2} < T_{U(1)}$. The low temperature regime $T < T_{Z_2}(I)$ has bistability with two possible steady states and history dependent IV curves. The different transitions could be observed experimentally with measurements of the transverse and longitudinal voltage.

We acknowledge H. Pastoriza and J. José for useful discussions and Fundación Antorchas and Conicet (Argentina) for financial support.

- [1] A. E. Koshelev and V. M. Vinokur, Phys. Rev. Lett. **73**, 3580 (1994); T. Giamarchi and P. Le Doussal, *ibid.* **76**, 3408 (1996); P. Le Doussal and T. Giamarchi, Phys. Rev. B **57**, 11356 (1998); S. Scheidl and V. M. Vinokur, *ibid.* **57**, 13800 (1998); L. Balents, M. C. Marchetti and L. Radzihovsky, *ibid.* **57**, 7705 (1998).
- [2] S. Bhattacharya and M. J. Higgins, Phys. Rev. Lett. **70**, 2617 (1993); F. Pardo *et al.*, Nature (London) **396**, 348 (1998).
- [3] K. Moon, R. T. Scalettar and G. Zimányi, Phys. Rev. Lett. **77**, 2778 (1996); S. Ryu *et al.*, *ibid.* **77**, 5114 (1996); N. Grønbech-Jensen, A. R. Bishop and D. Domínguez, *ibid.* **76**, 2985 (1996); C. Reichhardt *et al.*, *ibid.* **78**, 2648 (1997); C. J. Olson, C. Reichhardt and F. Nori, *ibid.* **81**, 3757 (1998); A. B. Kolton, D. Domínguez and N. Grønbech-Jensen, *ibid.* **83**, 3061 (1999).
- [4] L. Balents and M. P. A. Fisher, Phys. Rev. Lett. **75**, 4270 (1995).
- [5] For recent reviews see R. S. Newrock, C. J. Lobb, U. Geigenmuller and M. Octavio, Solid State Physics **54**, 263 (2000); *Lectures on superconducting networks and mesoscopic systems*, Ed. C. Giovannella and C. J. Lambert (American Institute of Physics, AIP Conf. Proc. 427, New York, 1998).
- [6] D. Domínguez, Phys. Rev. Lett. **72**, 3096 (1994) and **82**, 181 (1999).
- [7] V. I. Marconi and D. Domínguez, Phys. Rev. Lett. **82**, 4922 (1999), and Phys. Rev. B (2001).
- [8] S. Teitel and C. Jayaprakash, Phys. Rev. B **27**, 598 (1983); Phys. Rev. Lett. **51**, 199 (1983).
- [9] B. Berge *et al.*, Phys. Rev. B **34**, 3177 (1986).
- [10] B. J. van Wees, H. S. J. van der Zant, and J. E. Mooij, Phys. Rev. B **35**, 7291 (1987); Ph. Lerch *et al.*, *ibid.* **41**, 11479 (1990); H. S. J. van der Zant, H. A. Rijken, and J. E. Mooij, J. Low. Temp. Phys. **79**, 289 (1991).
- [11] K. K. Mon and S. Teitel, Phys. Rev. Lett. **62**, 673 (1989).
- [12] J. Lee, J. M. Kosterlitz, and E. Granato, Phys. Rev. B **43**, 11531 (1991); E. Granato *et al.*, Phys. Rev. Lett. **66**, 1090 (1991).
- [13] G. Ramirez-Santiago and J. V. José, Phys. Rev. Lett. **68**, 1224 (1992); Phys. Rev. B **49**, 9567 (1994).
- [14] P. Olsson, Phys. Rev. Lett. **75**, 2758 (1995).
- [15] M. Benakli and E. Granato, Phys. Rev. B **55**, 8361 (1997).
- [16] E. H. Boubecheur and H. T. Diep, Phys. Rev. B **58**, 5163 (1998).
- [17] J. S. Chung, K. H. Lee, and D. Stroud, Phys. Rev. B **40**, 6570 (1989); F. Falo *et al.*, *ibid.* **41**, 10983 (1990).
- [18] S. Kim and M. Y. Choi, Phys. Rev. B **48**, 322 (1993).
- [19] M. V. Simkin, Phys. Rev. B **57**, 7899 (1998).
- [20] M. S. Rzchowski *et al.*, Phys. Rev. B **42**, 2041 (1990).
- [21] B. J. Kim and P. Minnhagen, Phys. Rev. B **61**, 7017 (2000).
- [22] N. Grønbech-Jensen *et al.*, Phys. Rev. B **46**, 11149 (1992).
- [23] I. F. Marino, T. C. Halsey, Phys. Rev. B **50**, 6289 (1994).